

BCSJ Award Article

Ferromagnetic Interactions in Non-Kekulé Polymers. II[1]

Masashi Hatanaka* and Ryuichi Shiba

Department of Materials and Life Sciences, Graduate School of Advanced Science & Technology, Tokyo Denki University, 2-2 Kanda Nishiki-cho, Chiyoda-ku, Tokyo 101-8457

Received September 28, 2007; E-mail: mhatanaka@xug.biglobe.ne.jp

Ferromagnetic interactions in two-dimensional non-Kekulé polymers were theoretically analyzed under periodic boundary conditions. We constructed two-dimensional Wannier functions in the non-bonding crystal orbitals (NBCOs), and PNBCO (product of NBCO) were their products. Ferromagnetic interactions were attributed to anti-parallel-spin instabilities in PNBCO, similar to one-dimensional non-Kekulé polymers. The instabilities consisted of on-site terms and through-space terms. The former resulted from the squared amplitude of the same atomic site in PNBCO, and the latter resulted from antibonding-through-space interactions between second-nearest-neighbor carbon atomic sites in PNBCO.

There has been increasing interest in organic ferromagnets. Mataga theoretically proposed possible organic ferromagnets based on molecular orbital methods.[2] The theory is based on topological degeneracy[3] of non-bonding molecular orbitals (NBMOs) characteristic of non-Kekulé systems. In particular, *m*-phenylene (**1**) in Figure 1 has been regarded as a robust ferromagnetic coupler in organic ferromagnets.[2,3] The carbon atomic sites can be divided into two groups, that is, so-called starred atoms and unstarred atoms.[4] They can be chosen so as to be not adjacent each other. Then, the spin-quantum number of non-Kekulé systems predicted by Hund's rule becomes $(N_c - 2T)/2$, where N_c and T are the number of carbon atoms and classical double bonds, respectively.[4] Ovchinnikov also proposed possible organic ferromagnets based on non-Kekulé polymers in view of valence bond theory.[5] The spin-quantum number of non-Kekulé systems predicted by Ovchinnikov is $|n_A - n_{A+}|/2$, where n_A and n_{A+} are identical to the number of starred and unstarred atoms, respectively.[5] This theory has been related to the spin-polarization concept in non-Kekulé systems.[6] Tyutyulkov and co-workers also have designed many non-Kekulé polymers based on band theory.[7–9] A typical one-dimensional non-Kekulé polymer, poly(*m*-phenylene) (**2**), is shown in Figure 1. High-spin states of polymers and oligomers based on *m*-phenylene skeletons have been theoretically well established.[7,8,10–12] Thus, non-Kekulé chain polymers, including poly(*m*-phenylene), have been promising candidates for organic ferromagnets. Recent, heteroatom-containing systems have also been investigated due to their stabilities.[13–16]

Non-Kekulé chain polymers are extended systems of non-Kekulé molecules. High-spin non-Kekulé molecules have "nondisjoint" NBMOs[17,18] which span common atoms. The ferromagnetic spin alignment in non-Kekulé systems essentially results from an exchange integral between nondisjoint NBMOs.[19–21] Through-space interactions in nondisjoint systems also have been pointed out as another ferromagnetic interaction.[22] Similarly, possible organic ferromagnets based on non-Kekulé polymers have infinite NBMOs to form non-bonding crystal orbitals (NBCOs) which are nondisjoint.[1]

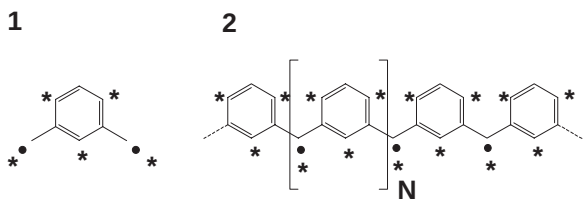

Figure 1. Molecular structures of *m*-phenylene (**1**) and poly(*m*-phenylene) (**2**).

Recently, ferromagnetic interactions in non-Kekulé systems have been interpreted in view of anti-parallel-spin instabilities in the product of NBMOs or NBCOs.[1,22] That is, triplet preference in non-Kekulé biradicals has been attributed to singlet instabilities in the product of NBMOs (PNBMO).[22] Moreover, ferromagnetic interactions in one-dimensional non-Kekulé polymers have been attributed to anti-parallel-spin instabilities in the products of NBCOs (PNBCO),[1] which is an extended concept of PNBMO. This situation is schematically shown in Figure 2. Figure 2 describes the construction of PNBMO in **1** and PNBCO in **2**. The PNBMO and PNBCO are products of maximally localized NBMOs and NBCOs, respectively.[1] It has been clarified that the origin of the ferromagnetic interactions are due to anti-parallel-spin instabilities in PNBMO or PNBCO. It has also been shown that the instabilities consist of on-site terms and through-space terms.[1] In one-dimensional non-Kekulé polymers, the former results from the squared amplitude of the same atomic site in PNBCO, and the latter results from antibonding-through-space interactions between second-nearest-neighbor carbon atomic sites in PNBCO.[1,22]

Published on the web April 10, 2008; doi:10.1246/bcsj.81.460

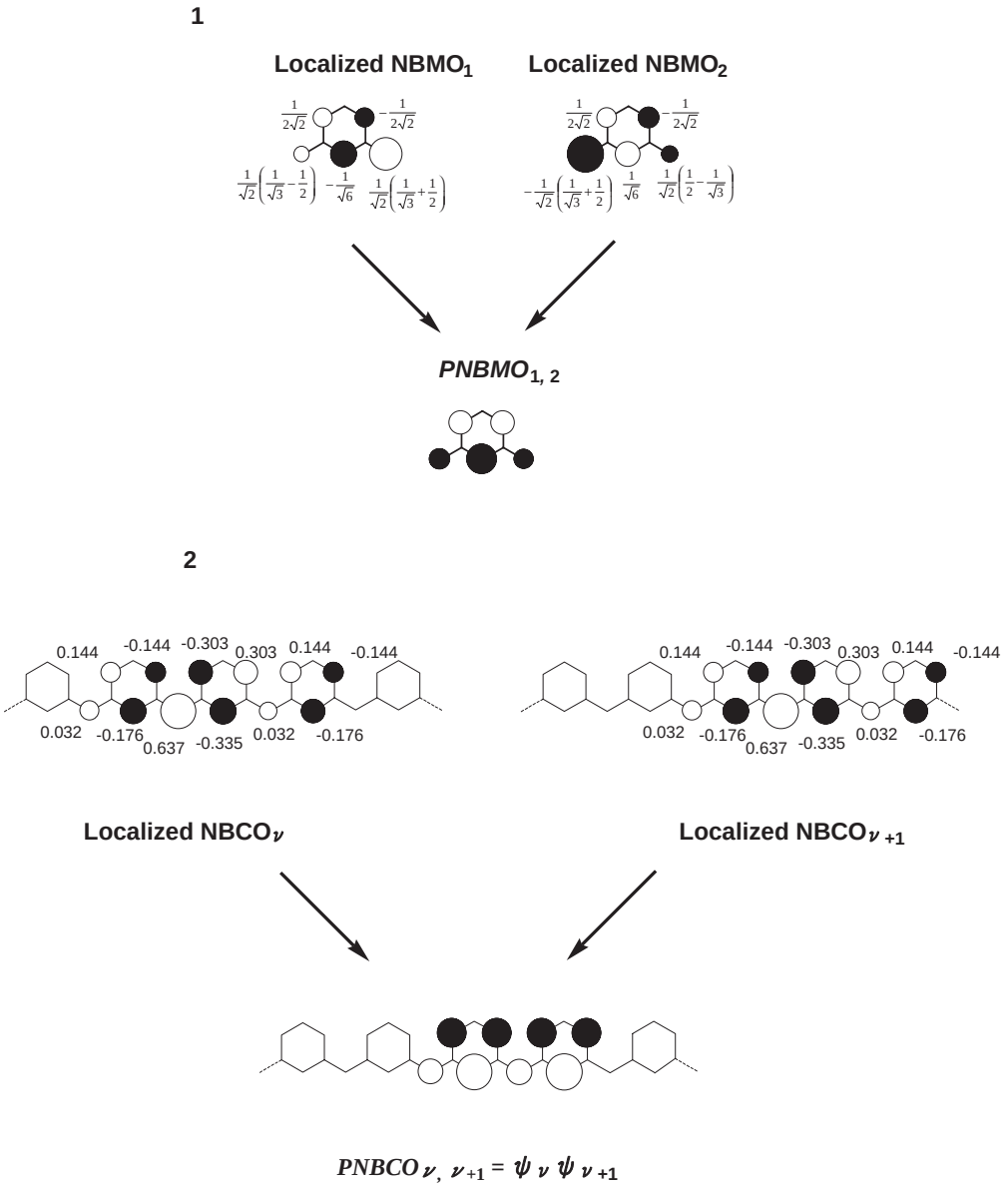

Figure 2. Construction of PNBMO in **1** and PNBCO in **2**.

However, in one-dimensional non-Kekulé polymers, defects in the polymers often destroy spin-coupling paths.[10] In order to overcome such a difficulty, two-dimensional non-Kekulé polymers with multiple spin-coupling paths have been suggested.[10,23,24] In two-dimensional non-Kekulé polymers, a few defects in the polymers do not significantly influence total spin-quantum number. In short, even if a certain spin-coupling pass is destroyed by a defect, the rest of the spin-coupling paths are still alive. Indeed, two-dimensional non-Kekulé polymers with very large spin-quantum numbers have been synthesized by using calixarenes.[23,24]

In this paper, the concept of PNBCO is expanded for two-dimensional non-Kekulé polymers by analyzing so-called Mataga polymer (**3**) described in Figure 3. **3** is one of the most promising candidates for two-dimensional organic ferromagnets with multiple spin-coupling paths.[10] The molecular structure contains a 1,3,5-benzenetriyl skeleton, which is also a robust ferromagnetic coupler.[25,26] We constructed Wannier functions of the NBCO and analyzed the amplitude pattern of the resultant PNBCO. It was shown that ferromagnetic interactions in two-dimensional non-Kekulé polymers were attributed to anti-parallel-spin instabilities in PNBCO. The spin-coupling paths originated from the on-site and through-space amplitude product of PNBCO, similar to one-dimensional non-Kekulé polymers. In order to describe the essential origin of the ferromagnetism in two-dimensional non-Kekulé polymers, theoretical formulation and qualitative descriptions of ferromagnetic interactions are shown.

Theoretical

The unit cell of **3** was defined as described in Figure 4. The numbers 1–7 in the unit cell are an index of the carbon atomic sites. $\boldsymbol{\mu}_1$ and $\boldsymbol{\mu}_2$ are principal lattice vectors. We first constructed Bloch functions of the NBCO. Although the Bloch functions of **3** have been reported in the literature,[8] they are complex solutions. The complex solutions of Bloch functions

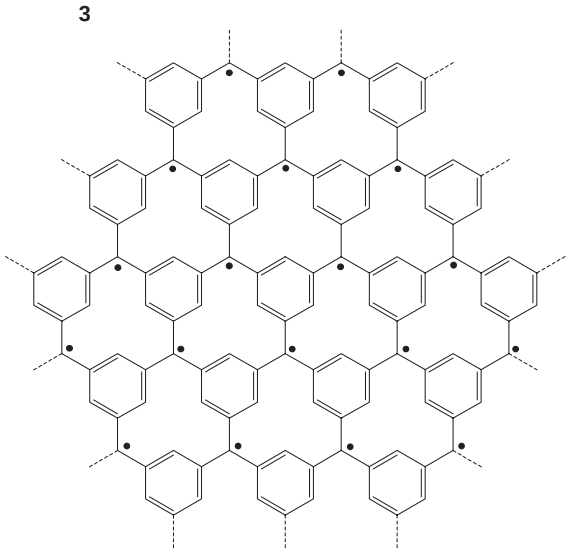

Figure 3. Molecular structure of Mataga polymer (**3**).

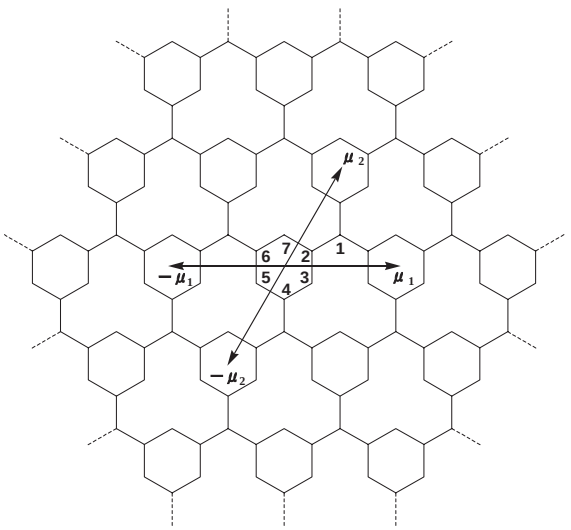

Figure 4. Definition of the unit cell and lattice vectors in **3**.

are inconvenient, because they do not make the corresponding Wannier functions to be symmetric with respect to the unit-cell-number difference.[1] Thus, we reconstructed the Bloch functions as follows.

The Bloch functions $\varphi(k_1, k_2)$ are expressed by using the NBCOs coefficients $C_r(k_1, k_2)$, which depend on wavenumber component k_1 and k_2 running $-\pi$ to π:

$$\varphi(k_1, k_2) = \frac{1}{\sqrt{N}} \sum_{\mu_1,\mu_2}^{N} \sum_{r}^{n} \times \exp(ik_1\mu_1 + ik_2\mu_2) C_r(k_1, k_2) \chi_{\mu_1,\mu_2,r}, \quad (1)$$

where μ and r are indices of unit cell and carbon atomic orbital therein, respectively. N and n are the number of unit cells and carbon atomic orbitals therein, respectively. χ represents the $2p_z$ atomic orbitals. In the case of **3**, r is from 1 to 7. The NBCO coefficients $C_r(k_1, k_2)$ are obtained by solving the secular equation as follows:

$$\begin{vmatrix} x & 1 & 0 & e^{ik_1} & 0 & e^{ik_2} & 0 \\ 1 & x & 1 & 0 & 0 & 0 & 1 \\ 0 & 1 & x & 1 & 0 & 0 & 0 \\ e^{-ik_1} & 0 & 1 & x & 1 & 0 & 0 \\ 0 & 0 & 0 & 1 & x & 1 & 0 \\ e^{-ik_2} & 0 & 0 & 0 & 1 & x & 1 \\ 0 & 1 & 0 & 0 & 0 & 1 & x \end{vmatrix} = 0, \quad (2)$$

where x is:

$$x = \frac{\alpha - \varepsilon}{\beta}. \quad (3)$$

α and β are Coulomb and resonance integrals, respectively. ε is orbital energy. The energy dispersion of the NBCO is:

$$x = 0. \quad (4)$$

Then, the NBCO coefficients $C_r(k_1, k_2)$ become:

$$C_1(k_1, k_2) = \frac{2}{\sqrt{13 - 2\cos k_1 - 2\cos k_2 - 2\cos(k_1 - k_2)}}, \quad (5)$$

$$C_3(k_1, k_2) = -\frac{1 - e^{-ik_1} + e^{-ik_2}}{\sqrt{13 - 2\cos k_1 - 2\cos k_2 - 2\cos(k_1 - k_2)}}, \quad (6)$$

$$C_5(k_1, k_2) = \frac{1 - e^{-ik_1} - e^{-ik_2}}{\sqrt{13 - 2\cos k_1 - 2\cos k_2 - 2\cos(k_1 - k_2)}}, \quad (7)$$

$$C_7(k_1, k_2) = -\frac{1 + e^{-ik_1} - e^{-ik_2}}{\sqrt{13 - 2\cos k_1 - 2\cos k_2 - 2\cos(k_1 - k_2)}}, \quad (8)$$

$$C_2(k_1, k_2) = C_4(k_1, k_2) = C_6(k_1, k_2) = 0. \quad (9)$$

We adopted the real part of each $C_r(k_1, k_2)$ as follows:

$$C'_r(k_1, k_2) = \frac{1}{2}\{C_r(k_1, k_2) + C_r(k_1, k_2)^*\}, \quad (10)$$

where $C_r(k_1, k_2)^*$ is the complex conjugate of $C_r(k_1, k_2)$. The corresponding Wannier functions are obtained by the following transformation:[8]

$$\psi(\nu_1, \nu_2) = \sum_{\mu_1,\mu_2}^{N} \sum_{r}^{n} a_r(\mu_1 - \nu_1, \mu_2 - \nu_2) \chi_{\mu_1,\mu_2,r}, \quad (11)$$

where $a_r(\mu_1 - \nu_1, \mu_2 - \nu_2)$ is:

$$a_r(\mu_1 - \nu_1, \mu_2 - \nu_2) = \frac{1}{4\pi^2} \int_{-\pi}^{\pi} \int_{-\pi}^{\pi} \exp\{i(\mu_1 - \nu_1)k_1 + i(\mu_2 - \nu_2)k_2\} C'_r(k_1, k_2) dk_1 dk_2, \quad (12)$$

in the limit of $N \to \infty$. The coefficient $a_r(\mu_1 - \nu_1, \mu_2 - \nu_2)$ depends only on the differences $(\mu_1 - \nu_1)$ and $(\mu_2 - \nu_2)$. We express $(\mu_1 - \nu_1)$ and $(\mu_2 - \nu_2)$ as τ_1 and τ_2:

$$\tau_1 = \mu_1 - \nu_1, \quad \tau_2 = \mu_2 - \nu_2. \quad (13)$$

Then, $a_r(\mu_1 - \nu_1, \mu_2 - \nu_2)$ is rewritten as:

$$a_r(\mu_1 - \nu_1, \mu_2 - \nu_2) = a_r(\tau_1, \tau_2). \quad (14)$$

τ_1 and τ_2 are the difference between the unit-cell number μ and ν. We note that each $a_r(\tau_1, \tau_2)$ is an even function with respect to τ_1 and τ_2, that is:

$$a_r(\tau_1, \tau_2) = a_r(-\tau_1, \tau_2), \quad (15)$$

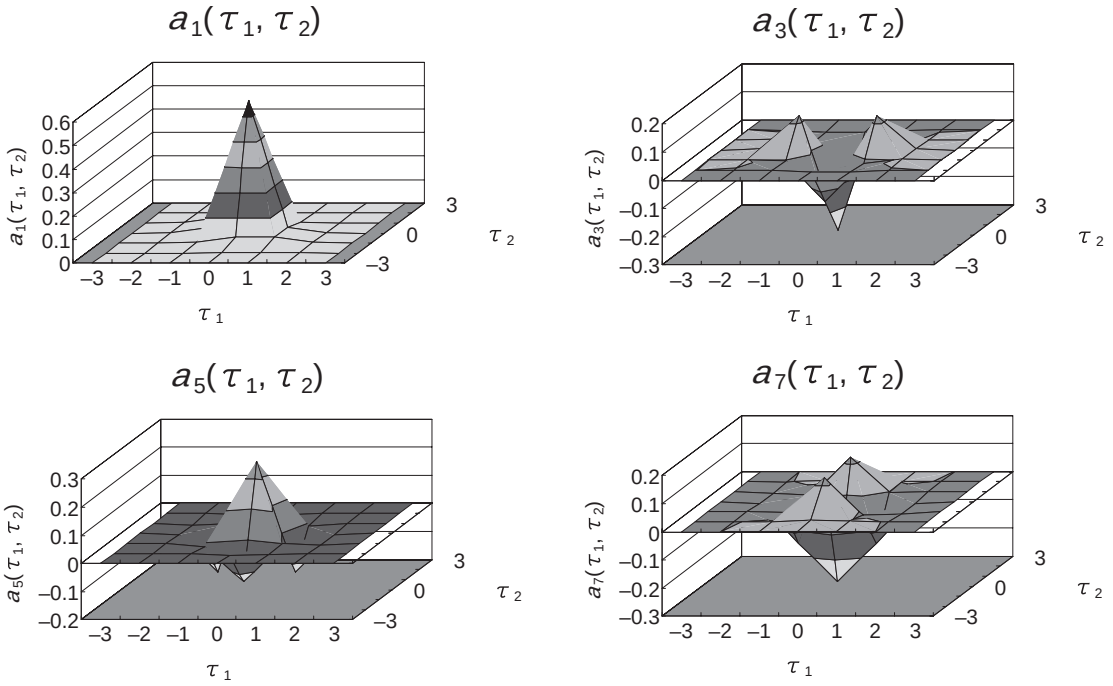

Figure 5. τ_1 and τ_2 dependence of each Wannier-function coefficient $a_r(\tau_1, \tau_2)$.

$$a_r(\tau_1, \tau_2) = a_r(\tau_1, -\tau_2). \tag{16}$$

This is guaranteed by eqs 10 and 12. $a_1(\tau_1, \tau_2)$ were calculated by numerical integration of the concrete expression:

$$a_1(\tau_1, \tau_2) = \frac{1}{4\pi^2}\int_{-\pi}^{\pi}\int_{-\pi}^{\pi}\frac{2\cos(\tau_1 k_1 + \tau_2 k_2)}{\sqrt{13 - 2\cos k_1 - 2\cos k_2 - 2\cos(k_1 - k_2)}}\mathrm{d}k_1\mathrm{d}k_2. \tag{17}$$

$a_2(\tau_1, \tau_2)$, $a_4(\tau_1, \tau_2)$, and $a_6(\tau_1, \tau_2)$ were zero:

$$a_2(\tau_1, \tau_2) = a_4(\tau_1, \tau_2) = a_6(\tau_1, \tau_2) = 0 \tag{18}$$

because $C_2(k_1, k_2)$, $C_4(k_1, k_2)$, and $C_6(k_1, k_2)$ were zero. $a_3(\tau_1, \tau_2)$, $a_5(\tau_1, \tau_2)$, and $a_7(\tau_1, \tau_2)$ were calculated by using following relations:

$$\begin{aligned} a_3(\tau_1, \tau_2) = &-\frac{1}{2}\{a_1(\tau_1, \tau_2)\} + \frac{1}{4}\{a_1(\tau_1 - 1, \tau_2) \\ &- a_1(\tau_1, \tau_2 - 1) + a_1(\tau_1 + 1, \tau_2) \\ &- a_1(\tau_1, \tau_2 + 1)\}, \end{aligned} \tag{19}$$

$$\begin{aligned} a_5(\tau_1, \tau_2) = &\frac{1}{2}\{a_1(\tau_1, \tau_2)\} - \frac{1}{4}\{a_1(\tau_1 - 1, \tau_2) \\ &+ a_1(\tau_1, \tau_2 - 1) + a_1(\tau_1 + 1, \tau_2) \\ &+ a_1(\tau_1, \tau_2 + 1)\}, \end{aligned} \tag{20}$$

$$\begin{aligned} a_7(\tau_1, \tau_2) = &-\frac{1}{2}\{a_1(\tau_1, \tau_2)\} + \frac{1}{4}\{-a_1(\tau_1 - 1, \tau_2) \\ &+ a_1(\tau_1, \tau_2 - 1) - a_1(\tau_1 + 1, \tau_2) \\ &+ a_1(\tau_1, \tau_2 + 1)\}. \end{aligned} \tag{21}$$

This is confirmed by eqs 5–12.

τ_1 and τ_2 dependence of $a_r(\tau_1, \tau_2)$ in **3** are shown in Figure 5. We can see that each $a_r(\tau_1, \tau_2)$ ($r = 1$, 3, 5, and 7) decreases when the norm of the vector-type index (τ_1, τ_2) increases. In fact, $a_r(\tau_1, \tau_2)$ with $|(\tau_1, \tau_2)|^2 = {\tau_1}^2 + {\tau_2}^2 \geq 2$ are trivial compared with $a_r(0, 0)$, $a_r(\pm 1, 0)$, and $a_r(0, \pm 1)$. That is:

$$\begin{aligned} 0 < \ldots |a_r(-3, 0)| < |a_r(-2, 0)| \ll |a_r(-1, 0)| < |a_r(0, 0)| \\ > |a_r(1, 0)| \gg |a_r(2, 0)| > |a_r(3, 0)| \ldots > 0, \end{aligned} \tag{22}$$

$$\begin{aligned} 0 < \ldots |a_r(0, -3)| < |a_r(0, -2)| \ll |a_r(0, -1)| < |a_r(0, 0)| \\ > |a_r(0, 1)| \gg |a_r(0, 2)| > |a_r(0, 3)| \ldots > 0. \end{aligned} \tag{23}$$

Therefore, we supposed that:

$$a_r(\tau_1, \tau_2) = 0 \quad \text{when} \quad |(\tau_1, \tau_2)|^2 \geq 2. \tag{24}$$

Each $a_r(\tau_1, \tau_2)$ ($r = 1$–7) rapidly decays when $|(\tau_1, \tau_2)| \geqq 2$. As a result, the (ν_1, ν_2)-th Wannier function is localized at (ν_1, ν_2)-th, $(\nu_1 \pm 1, \nu_2)$-th, and $(\nu_1, \nu_2 \pm 1)$-th cells. The schematic representation of the (ν_1, ν_2)-th Wannier function is given in Figure 6. Similarly, the $(\nu_1 \pm 1, \nu_2)$-th and the $(\nu_1, \nu_2 \pm 1)$-th Wannier functions are obtained by translation. As is shown later, products between these Wannier functions are formulated as two-electron wave function PNBCOs, and play essential roles in ferromagnetic interactions.

The electronic configuration of the ferromagnetic state of polymer **3** by using the Wannier functions is described in Figure 7. Since simultaneous occupancy of two electrons with parallel spin at the same Wannier function is forbidden by the Pauli principle, ferromagnetic interactions occur between two Wannier functions with different index pair (ν_1, ν_2). The pairs of indices which make PNBCOs not to vanish are $\{(\nu_1, \nu_2), (\nu_1 + 1, \nu_2)\}$, $\{(\nu_1, \nu_2), (\nu_1 - 1, \nu_2)\}$, $\{(\nu_1, \nu_2), (\nu_1, \nu_2 + 1)\}$, and $\{(\nu_1, \nu_2), (\nu_1, \nu_2 - 1)\}$. This is confirmed

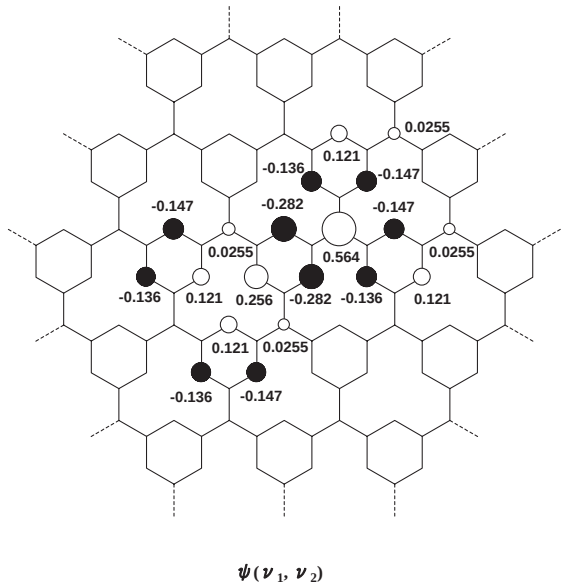

Figure 6. Schematic representation of Wannier function $\psi(\nu_1, \nu_2)$ in **3**.

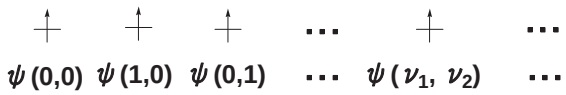

Figure 7. Electronic configuration of ferromagnetic state in **3**.

by eq 24. We denote the corresponding PNBCOs as $PNBCO\{(\nu_1, \nu_2), (\nu_1 + 1, \nu_2)\}$, $PNBCO\{(\nu_1, \nu_2), (\nu_1 - 1, \nu_2)\}$, $PNBCO\{(\nu_1, \nu_2), (\nu_1, \nu_2 + 1)\}$, and $PNBCO\{(\nu_1, \nu_2), (\nu_1, \nu_2 - 1)\}$. Considering the symmetry of the system, these four PNBCOs essentially have the same amplitude pattern. Thus, for a while, we focused only on the amplitude pattern of $PNBCO\{(\nu_1, \nu_2), (\nu_1 + 1, \nu_2)\}$ as follows.

We constructed a two-electron wave function by product of the (ν_1, ν_2)-th and $(\nu_1 + 1, \nu_2)$-th Wannier functions as $PNBCO\{(\nu_1, \nu_2), (\nu_1 + 1, \nu_2)\}$:

$$
\begin{aligned}
&PNBCO\{(\nu_1, \nu_2), (\nu_1 + 1, \nu_2)\} = \psi(\nu_1, \nu_2)(\mathbf{1})\psi(\nu_1 + 1, \nu_2)(\mathbf{2}) \\
&= \left(\sum_{\mu_1, \mu_2}^{N} \sum_{r}^{n} a_r(\mu_1 - \nu_1, \mu_2 - \nu_2)\chi_{\mu_1, \mu_2, r}(\mathbf{1}) \right) \\
&\quad \times \left(\sum_{\mu'_1, \mu'_2}^{N} \sum_{s}^{n} a_s(\mu'_1 - \nu_1 - 1, \mu'_2 - \nu_2)\chi_{\mu'_1, \mu'_2, s}(\mathbf{2}) \right) \\
&= \left(\sum_{\tau_1 + \nu_1, \tau_2}^{N} \sum_{r}^{n} a_r(\tau_1, \tau_2)\chi_{\tau_1 + \nu_1, \nu_2, r}(\mathbf{1}) \right) \\
&\quad \times \left(\sum_{\tau'_1 + \nu'_1, \tau'_2}^{N} \sum_{s}^{n} a_s(\tau'_1 - 1, \tau'_2)\chi_{\tau'_1 + \nu_1, \nu_2, s}(\mathbf{2}) \right) \\
&\cong \left(\sum_{\tau_1, \tau_2}^{(-1,0),(0,0),(1,0)} \sum_{r}^{n} a_r(\tau_1, \tau_2)\chi_{\tau_1 + \nu_1, \nu_2, r}(\mathbf{1}) \right) \\
&\quad \times \left(\sum_{\tau'_1, \tau'_2}^{(0,0),(1,0),(2,0)} \sum_{s}^{n} a_s(\tau'_1 - 1, \tau'_2)\chi_{\tau'_1 + \nu_1, \nu_2, s}(\mathbf{2}) \right) \\
&= \left[\sum_{r}^{n} \{a_r(-1, 0)\chi_{\nu_1 - 1, \nu_2, r}(\mathbf{1}) + a_r(0, 0)\chi_{\nu_1, \nu_2, r}(\mathbf{1}) \right. \\
&\quad \left. + a_r(1, 0)\chi_{\nu_1 + 1, \nu_2, r}(\mathbf{1})\} \right] \times \left[\sum_{s}^{n} \{a_s(-1, 0)\chi_{\nu_1, \nu_2, s}(\mathbf{2}) \right. \\
&\quad \left. + a_s(0, 0)\chi_{\nu_1 + 1, \nu_2, s}(\mathbf{2}) + a_s(1, 0)\chi_{\nu_1 + 2, \nu_2, s}(\mathbf{2})\} \right], \qquad (25)
\end{aligned}
$$

where Equation 24 was applied in the approximation. The electron numbers "**1**" and "**2**" were added by bold letters for clarification. Equation 25 is further approximated under "neglect of differential overlap" (NDO approximation) as follows:

$$
\begin{aligned}
&PNBCO\{(\nu_1, \nu_2), (\nu_1 + 1, \nu_2)\} = \psi(\nu_1, \nu_2)(\mathbf{1})\psi(\nu_1 + 1, \nu_2)(\mathbf{2}) \\
&\cong C \left[\sum_{r}^{(\nu_1, \nu_2)\text{-th cell}} \{a_r(-1, 0)a_r(0, 0)\chi_{\nu_1, \nu_2, r}(\mathbf{1})\chi_{\nu_1, \nu_2, r}(\mathbf{2})\} \right. \\
&\quad \left. + \sum_{r}^{(\nu_1 + 1, \nu_2)\text{-th cell}} \{a_r(0, 0)a_r(1, 0)\chi_{\nu_1 + 1, \nu_2, r}(\mathbf{1})\chi_{\nu_1 + 1, \nu_2, r}(\mathbf{2})\} \right] \\
&= C \left[\sum_{r}^{(\nu_1, \nu_2)\text{-th cell}} \{a_r(0, 0)a_r(1, 0)\chi_{\nu_1, \nu_2, r}(\mathbf{1})\chi_{\nu_1, \nu_2, r}(\mathbf{2})\} \right. \\
&\quad \left. + \sum_{r}^{(\nu_1 + 1, \nu_2)\text{-th cell}} \{a_r(0, 0)a_r(1, 0)\chi_{\nu_1 + 1, \nu_2, r}(\mathbf{1})\chi_{\nu_1 + 1, \nu_2, r}(\mathbf{2})\} \right]. \qquad (26)
\end{aligned}
$$

In the last expression, even-function character of $a_r(\tau)$ (eq 15) was applied. We note that the first and second summations in the last expression are taken in the (ν_1, ν_2)-th and $(\nu_1 + 1, \nu_2)$-th cell, respectively. C is chosen so that the PNBCO is normalized under the NDO approximation. That is:

$$
C = \frac{1}{\sqrt{\sum_{r}^{(\nu_1, \nu_2)\text{-th cell}} \{a_r(0, 0)^2 a_r(1, 0)^2\} + \sum_{r}^{(\nu_1 + 1, \nu_2)\text{-th cell}} \{a_r(0, 0)^2 a_r(1, 0)^2\}}}. \qquad (27)
$$

NDO approximation is suitable for description of electronic states in non-Kekulé systems.[1,22] The last expression in eq 26 makes it possible to obtain schematic representation of PNBCO by simple product between the coefficients on the same atomic site in the (ν_1, ν_2)-th and $(\nu_1 + 1, \nu_2)$-th cells.

Figure 8a shows amplitude patterns of Wannier functions $\psi(\nu_1, \nu_2)$, $\psi(\nu_1 + 1, \nu_2)$, and $PNBCO\{(\nu_1, \nu_2), (\nu_1 + 1, \nu_2)\}$ of **3**. The PNBCO is created along the lattice vector $\boldsymbol{\mu}_1$. Figure 8b similarly shows $\psi(\nu_1, \nu_2)$, $\psi(\nu_1, \nu_2 + 1)$, and the corresponding product $PNBCO\{(\nu_1, \nu_2), (\nu_1, \nu_2 + 1)\}$. In this case, the PNBCO is created along the lattice vector $\boldsymbol{\mu}_2$, and the amplitude pattern is essentially the same as Figure 8a. Since NDO

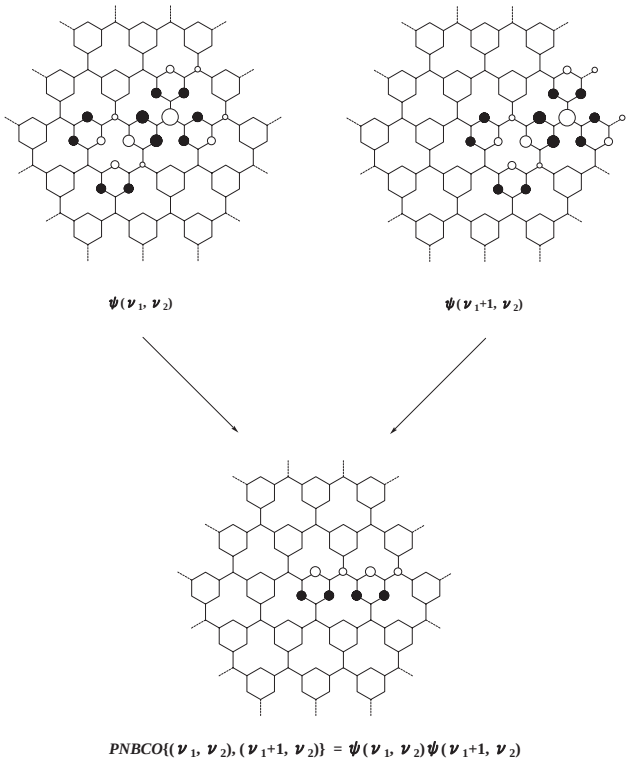

(a)

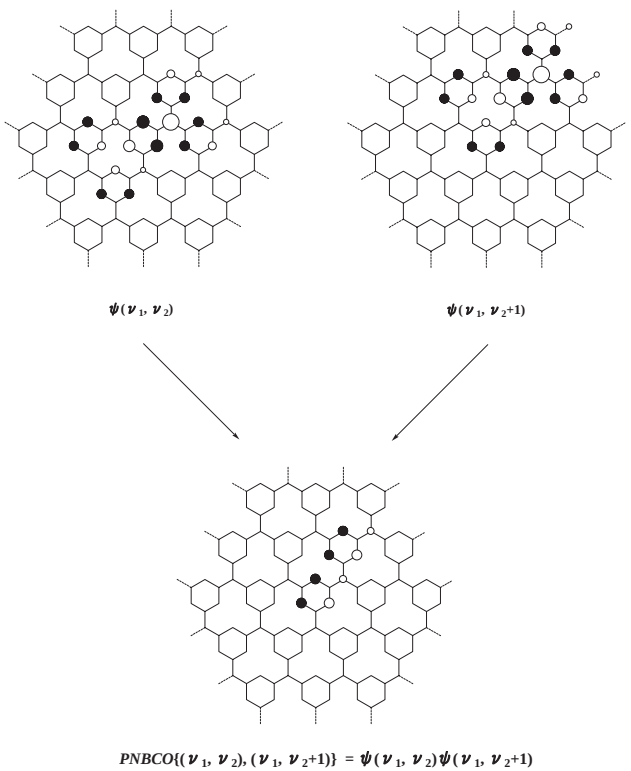

(b)

Figure 8. (a) PNBCO created along the lattice vector $\boldsymbol{\mu}_1$. (b) PNBCO created along the lattice vector $\boldsymbol{\mu}_2$.

approximation was applied, each PNBCO contained only ionic terms. Therefore, the squared amplitudes of the PNBCOs represent instabilities of anti-parallel-spin states. In short, since simultaneous occupancy of two electrons with parallel spin in the same atomic orbital is forbidden by the Pauli principle, resultant reduction of Coulomb repulsion leads to parallel-spin preference in PNBCOs. This situation resembles that in nondisjoint biradicals[22] and one-dimensional non-Kekulé polymers,[1] in which the squared amplitudes of the PNBMO or PNBCO represent anti-parallel-spin instabilities.

In nondisjoint-type biradicals, apart from the normalization factor, the sum of the squared amplitudes of PNBMO is approximately proportional to the exchange integral between two NBMOs.[19,22] Similarly, nondisjoint-type chain polymers have been predicted to be ferromagnetic, and the sum of the squared amplitudes of PNBCO divided by the normalization factor is approximately proportional to the exchange integral between the NBCOs.[1] Such a consideration also holds in two-dimensional PNBCOs described above. For example, $|PNBCO\{(\nu_1, \nu_2), (\nu_1 + 1, \nu_2)\}|/C^2 = 1/C^2$ is also considered to be approximately proportional to the exchange integral between the two Wannier functions $\psi(\nu_1, \nu_2)$ and $\psi(\nu_1 + 1, \nu_2)$. This is consistent with recent studies of high-spin oligomers and/or polymers using the L_{ij} index.[19–21] L_{ij} index is approximately proportional to the exchange integral between NBMOs of polyradicals.[19–21] Although the L_{ij} index has been defined in oligomers and expanded for polymers by extrapolation,[19–21] The PNBCO described above is formulated in infinite systems under two-dimensional periodic boundary conditions.

Next, we explain through-space interactions in PNBCO. It is shown that antibonding through-space interactions in PNBCO stabilize the ferromagnetic state. The PNBCO of **3** contains in-phase and out-of-phase moieties between the second-nearest-neighbor atomic sites as depicted in Figure 9. In Figure 9, $PNBCO\{(\nu_1, \nu_2), (\nu_1 + 1, \nu_2)\}$ and $PNBCO\{(\nu_1, \nu_2), (\nu_1, \nu_2 + 1)\}$ are shown corresponding to Figure 8a and Figure 8b, respectively. The in-phase and out-of-phase moieties were described as "P_{sym}-fragment" and "P_{anti}-fragment," respectively. The anti-parallel-spin states are stabilized by P_{sym}-fragments and destabilized by P_{anti}-fragments, analogous to through-space interactions in nondisjoint biradicals.[22] At least one P_{anti}-fragments always appears around the "unstarred atoms" which have no amplitudes. This is due to linkage of starred atoms to unstarred atoms and resultant orbital mixing.[22] Then, PNBCO becomes antibonding rich. We can see that the number of P_{anti}-fragments is larger than that of P_{sym}-fragments. This situation has been clarified by using unitary transformation of NBMOs.[22] In addition, it has been shown that the destabilization energy by P_{anti}-fragments is larger than the stabilization energy by P_{sym}-fragments.[22] Therefore, in non-Kekulé polymers, through-space interactions in P_{anti}-fragments are more significant than those in P_{sym}-fragments.[1] In the next section, the through-space interactions are formulated by introducing an overlap integral into PNBCO.

Discussion

Through-space interactions in PNBCO are formulated taking account of overlap integral, because the interactions occur between non-nearest-neighbor carbon atomic sites. Of all

non-nearest-neighbor carbon atomic sites, only second-nearest-neighbor carbon atomic sites are important.[22] We analyze through-space interactions in $PNBCO\{(\nu_1,\nu_2),(\nu_1+1,\nu_2)\}$ defined above. Taking account of overlap integral s_{st} between atomic site s and t, $PNBCO\{(\nu_1,\nu_2),(\nu_1+1,\nu_2)\}$ in eq 26 is extended as follows:

$$\begin{aligned} PNBCO\{(\nu_1,\nu_2),(\nu_1+1,\nu_2)\} &= \psi(\nu_1,\nu_2)(\mathbf{1})\psi(\nu_1+1,\nu_2)(\mathbf{2}) \\ &\cong \frac{C\left[\sum_r^{(\nu_1,\nu_2)\text{-th cell}} \{a_r(0,0)a_r(1,0)\chi_{\nu_1,\nu_2,r}(\mathbf{1})\chi_{\nu_1,\nu_2,r}(\mathbf{2})\} + \sum_r^{(\nu_1+1,\nu_2)\text{-th cell}} \{a_r(0,0)a_r(1,0)\chi_{\nu_1+1,\nu_2,r}(\mathbf{1})\chi_{\nu_1+1,\nu_2,r}(\mathbf{2})\}\right]}{\sqrt{1+Z\{(\nu_1,\nu_2),(\nu_1+1,\nu_2)\}}}, \end{aligned} \tag{28}$$

where $Z\{(\nu_1,\nu_2),(\nu_1+1,\nu_2)\}$ is:

$$Z\{(\nu_1,\nu_2),(\nu_1+1,\nu_2)\} = 2C^2\left[\begin{array}{l} \sum_{s\neq t}^{(\nu_1,\nu_2)\text{-th cell}} a_s(0,0)a_s(1,0)a_t(0,0)a_t(1,0)+ \\ \sum_{s\neq t}^{(\nu_1+1,\nu_2)\text{-th cell}} a_s(0,0)a_s(1,0)a_t(0,0)a_t(1,0)+ \\ \sum_{s\neq t}^{(\nu_1,\nu_2)\text{-th cell and }(\nu_1+1,\nu_2)\text{-th cell}} a_s(0,0)a_s(1,0)a_t(0,0)a_t(1,0) \end{array}\right] {s_{st}}^2. \tag{29}$$

Then, square of $PNBCO\{(\nu_1,\nu_2),(\nu_1+1,\nu_2)\}$ becomes:

$$\begin{aligned} PNBCO\{(\nu_1,\nu_2),(\nu_1+1,\nu_2)\}^2 &\cong [1+Z\{(\nu_1,\nu_2),(\nu_1+1,\nu_2)\}]^{-1} \\ &\times C\left[\sum_r^{(\nu_1,\nu_2)\text{-th cell}} \{a_r(0,0)a_r(1,0)\chi_{\nu_1,\nu_2,r}(\mathbf{1})\chi_{\nu_1,\nu_2,r}(\mathbf{2})\} + \sum_r^{(\nu_1+1,\nu_2)\text{-th cell}} \{a_r(0,0)a_r(1,0)\chi_{\nu_1+1,\nu_2,r}(\mathbf{1})\chi_{\nu_1+1,\nu_2,r}(\mathbf{2})\}\right] \\ &\times C\left[\sum_s^{(\nu_1,\nu_2)\text{-th cell}} \{a_s(0,0)a_s(1,0)\chi_{\nu_1,\nu_2,s}(\mathbf{1})\chi_{\nu_1,\nu_2,s}(\mathbf{2})\} + \sum_s^{(\nu_1+1,\nu_2)\text{-th cell}} \{a_s(0,0)a_s(1,0)\chi_{\nu_1+1,\nu_2,s}(\mathbf{1})\chi_{\nu_1+1,\nu_2,s}(\mathbf{2})\}\right] \\ &\cong C^2[1-Z\{(\nu_1,\nu_2),(\nu_1+1,\nu_2)\}] \\ &\times \left[\begin{array}{l} \sum_r^{(\nu_1,\nu_2)\text{-th cell}} \{a_r(0,0)^2a_r(1,0)^2\chi_{\nu_1,\nu_2,r}(\mathbf{1})^2\chi_{\nu_1,\nu_2,r}(\mathbf{2})^2\}+ \\ \sum_r^{(\nu_1+1,\nu_2)\text{-th cell}} \{a_r(0,0)^2a_r(1,0)^2\chi_{\nu_1+1,\nu_2,r}(\mathbf{1})^2\chi_{\nu_1+1,\nu_2,r}(\mathbf{2})^2\} \end{array}\right], \end{aligned} \tag{30}$$

under the NDO approximation. The term $[1-Z\{(\nu_1,\nu_2),(\nu_1+1,\nu_2)\}]$ resulted from Taylor expansion with respect to $Z\{(\nu_1,\nu_2),(\nu_1+1,\nu_2)\}$.

In eq 29, the first and second summations are taken in the (ν_1,ν_2) and (ν_1+1,ν_2)-th cell, respectively, and the third summation is taken between the (ν_1,ν_2) and (ν_1+1,ν_2)-th cells. In $Z\{(\nu_1,\nu_2),(\nu_1+1,\nu_2)\}$, the term $a_s(0,0)a_s(1,0)a_t(0,0)a_t(1,0)$ is the product of the s-th and t-th PNBCO amplitudes. This term is positive when the s-th and t-th PNBCO amplitudes have the same sign. Conversely, the term is negative when the s-th and t-th PNBCO amplitudes have different signs. Therefore, the term $a_s(0,0)a_s(1,0)a_t(0,0)a_t(1,0)$ is positive in P_{sym}-fragments and negative in P_{anti}-fragments, respectively. That is:

$$a_s(0,0)a_s(1,0)a_t(0,0)a_t(1,0) > 0 \quad \text{in } P_{\text{sym}}\text{-fragment}, \tag{31}$$

$$a_s(0,0)a_s(1,0)a_t(0,0)a_t(1,0) < 0 \quad \text{in } P_{\text{anti}}\text{-fragment}. \tag{32}$$

The number of P_{anti}-fragments is larger than that of P_{sym}-fragments, as described above. This is characteristic of nondisjoint systems,[1,22] and through-space interactions in PNBCO become antibonding rich. Therefore, $Z\{(\nu_1,\nu_2),(\nu_1+1,\nu_2)\}$ is negative and:

$$1-Z\{(\nu_1,\nu_2),(\nu_1+1,\nu_2)\} > 1. \tag{33}$$

Thus, from eq 30, degree of anti-parallel-spin instabilities, that is, squared amplitude of PNBCO increases by antibonding-through-space interactions.

Then, total instabilities in anti-parallel-spin states of PNBCO consist of on-site terms and through-space terms, similar to one-dimensional non-Kekulé polymers. The on-site term corresponds to squared amplitude of the same atomic site on PNBCO, and the through-space term corresponds to antibonding-through-space interactions due to $Z\{(\nu_1,\nu_2),(\nu_1+1,\nu_2)\}$ in PNBCO. This situation is expressed as follows:

$$\begin{aligned} |PNBCO|^2 \cong\ & |PNBCO|^2 \text{ (on-site term)} \\ & + |PNBCO|^2 \text{ (through-space term)}. \end{aligned} \tag{34}$$

Both on-site and through-space terms lead to parallel-spin preference, because they represent anti-parallel-spin instabilities, as described above.

That is, spin-coupling paths in two-dimensional non-Kekulé polymers are guaranteed by on-site and antibonding-through-space amplitude product in PNBCOs, which are created along the principal lattice vectors. The PNBCO analysis described

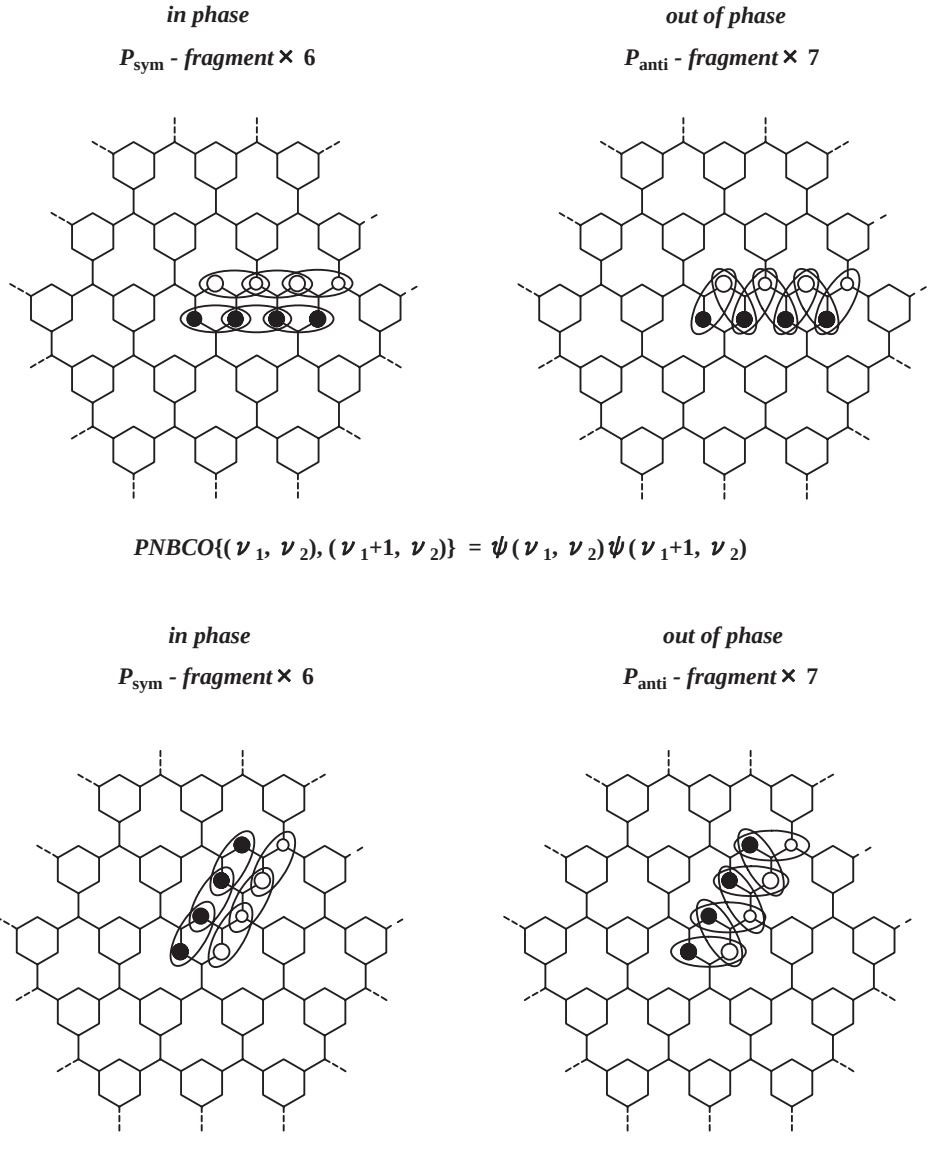

Figure 9. Through-space interactions in PNBCOs of **3**.

above will hold in general two-dimensional non-Kekulé polymers, because the PNBCOs are similarly created along the principal lattice vectors.

Conclusion

Ferromagnetic interactions in two-dimensional non-Kekulé polymers were theoretically analyzed under periodic boundary conditions. We constructed two-dimensional Wannier functions in the non-bonding crystal orbitals (NBCOs), and PNBCO (product of NBCO) was their product. The ferromagnetic interactions were attributed to anti-parallel-spin instabilities in the PNBCO. The instabilities consisted of on-site terms and through-space terms. The former resulted from the squared amplitude of the same atomic site in PNBCO, and the latter resulted from antibonding-through-space interactions between second-nearest-neighbor carbon atomic sites in PNBCO, similar to one-dimensional non-Kekulé polymers.

References

1 First communication: M. Hatanaka, R. Shiba, *Bull. Chem. Soc. Jpn.* **2007**, *80*, 2342.
2 N. Mataga, *Theor. Chim. Acta* **1968**, *10*, 372.
3 K. Itoh, *Pure Appl. Chem.* **1978**, *50*, 1251.
4 H. C. Longuet-Higgins, *J. Chem. Phys.* **1950**, *18*, 265.
5 A. A. Ovchinnikov, *Theor. Chim. Acta* **1978**, *47*, 297.
6 K. Yamaguchi, Y. Toyoda, T. Fueno, *Synth. Met.* **1987**, *19*, 81.
7 N. Tyutyulkov, P. Schuster, O. Polansky, *Theor. Chim. Acta* **1983**, *63*, 291.
8 N. N. Tyutyulkov, S. C. Karabunarliev, *Int. J. Quantum Chem.* **1986**, *29*, 1325.
9 F. Dietz, N. Tyutyulkov, *Chem. Phys.* **2001**, *264*, 37.
10 A. Rajca, *Chem. Rev.* **1994**, *94*, 871.
11 K. Yoshizawa, T. Kuga, T. Sato, M. Hatanaka, K. Tanaka, T. Yamabe, *Bull. Chem. Soc. Jpn.* **1996**, *69*, 3443.

12 H. Iwamura, *Adv. Phys. Org. Chem.* **1990**, *26*, 179.
13 H. Murata, D. Miyajima, R. Takada, H. Nishide, *Polym. J.* **2005**, *37*, 818.
14 T. Kurata, Y. J. Pu, H. Nishide, *Polym. J.* **2007**, *39*, 675.
15 M. Hatanaka, R. Shiba, *J. Comput. Chem., Jpn.* **2005**, *4*, 101.
16 M. Hatanaka, R. Shiba, *J. Comput. Chem., Jpn.* **2006**, *5*, 171.
17 W. T. Borden, E. R. Davidson, *J. Am. Chem. Soc.* **1977**, *99*, 4587.
18 W. T. Borden, *Mol. Cryst. Liq. Cryst.* **1993**, *232*, 195.
19 Y. Aoki, A. Imamura, *Int. J. Quantum Chem.* **1999**, *74*, 491.
20 Y. Orimoto, T. Imai, K. Naka, Y. Aoki, *J. Phys. Chem. A* **2006**, *110*, 5803.
21 Y. Orimoto, Y. Aoki, *J. Chem. Theory Comput.* **2006**, *2*, 786.
22 M. Hatanaka, R. Shiba, *Bull. Chem. Soc. Jpn.* **2007**, *80*, 1750.
23 A. Rajca, J. Wongsriratanakul, S. Rajca, *Science* **2001**, *294*, 1503.
24 S. Rajca, A. Rajca, *J. Solid State Chem.* **2001**, *159*, 460.
25 K. Yoshizawa, M. Hatanaka, A. Ito, K. Tanaka, T. Yamabe, *Chem. Phys. Lett.* **1993**, *202*, 483.
26 K. Yoshizawa, M. Hatanaka, Y. Matsuzaki, K. Tanaka, T. Yamabe, *J. Chem. Phys.* **1994**, *100*, 4453.